

Bulk-flow and β_I from the SMAC project

Russell J. Smith¹, Michael J. Hudson², John R. Lucey¹,
David J. Schlegel³ and Roger L. Davies¹

¹ *Department of Physics, University of Durham, Science Laboratories,
South Road, Durham, DH1 3LE, United Kingdom.*

² *Department of Physics & Astronomy, University of Victoria,
PO Box 3055, Victoria BC V8W 3PN, Canada.*

³ *Department of Astrophysical Sciences, Princeton University,
Peyton Hall, Princeton NJ, USA.*

Abstract. The SMAC project is a Fundamental Plane peculiar velocity survey of 56 clusters of galaxies to a depth of $cz \sim 12000 \text{ km s}^{-1}$. We present here some results from the analysis of the SMAC velocity field, focussing on three specific features: the best-fitting bulk-flow model for the SMAC data; the agreement between the observed velocity field and predictions from the IRAS-PSCz redshift survey; the role of the Great Attractor and Shapley Concentration in generating the local flows. We argue that the local mass distribution, as probed by the PSCz, can fully account for the observed cluster velocities.

1. Introduction

The ‘Streaming Motions of Abell Clusters’ (SMAC) project is a Fundamental Plane (FP) survey of ~ 700 early-type galaxies in 56 local rich clusters. The cluster sample has approximately full-sky coverage, and a limiting depth of $\sim 12000 \text{ km s}^{-1}$. Within each cluster, distances are based upon data for 4–56 E/S0 galaxies. Data for the SMAC project is drawn from a compilation of literature sources and an extensive body of new observations, carefully combined into a homogeneous database. Further details of the sample, the observations, and the data compilation procedures are reported by Hudson et al. (1999) and in a forthcoming series of papers.

Our (inverse) FP analysis closely follows the methods employed, for a smaller sample of clusters, by Hudson et al. (1997). The FP yields distances to a precision of $\sim 20\%$ per galaxy, so that cluster distances are determined with errors of 3–12%, with a median 8%. The velocity zero-point is calibrated by requiring that the sample exhibit no net radial inflow or outflow. The balanced sky-coverage of the sample ensures that there is little covariance between monopole and dipole components of the velocity field. The observed velocity field is presented in the upper panel of Figure 1. Lucey et al. (in this volume) present some example comparisons of the SMAC distances/velocities with those determined from other surveys with clusters in common (eg Lauer & Postman

1994; Dale et al. 1999). Such comparisons generally reveal an acceptable level of agreement, in so much as the scatter is compatible with the quoted errors. However, the distance errors are such that cluster-by-cluster comparisons are rather crude tests for systematic effects in distance estimates.

2. The SMAC bulk-flow

The best-fitting bulk-flow model is the vector \mathbf{V}_B which minimizes

$$\chi^2 = \sum_i \frac{(v_i - \mathbf{V}_B \cdot \hat{\mathbf{r}}_i)^2}{\sigma_i^2 + \sigma_{\text{th}}^2}, \quad (1)$$

where v_i is the observed radial peculiar velocity for cluster i , whose direction vector is $\hat{\mathbf{r}}_i$. The weights are assigned according to the observational peculiar velocity error, σ_i , and a ‘thermal’ velocity noise σ_{th} , here fixed at 250 km s^{-1} . In what follows, we shall refer to \mathbf{V}_B as ‘the bulk-flow’, but this terminology should be understood as a shorthand for ‘the best-fitting bulk-flow model’. As demonstrated by Feldman & Watkins (1994) and further illustrated by Hudson et al. (this volume), the incomplete cancellation of small- and intermediate-scale flows causes bulk-flow measurements to depend upon the sample geometry, characterised by the survey window function. This effect is especially important when the spatial sampling is sparse, as for cluster surveys.

For the SMAC sample, we determine the following CMB-frame bulk-flow solution:

$$\mathbf{V}_B^{\text{obs}} = [-345 \pm 85, +37 \pm 101, -538 \pm 158] \text{ km s}^{-1} \quad (2)$$

in supergalactic cartesian co-ordinates (used throughout this paper for flow vector components). After correcting for ‘error-biasing’, this vector has magnitude $640 \pm 200 \text{ km s}^{-1}$ and is directed towards $(l, b) = (260^\circ, -2^\circ)$. Note that the error ellipsoid is anisotropic, as demonstrated by Monte-Carlo simulations in the lower panel of Figure 1. The bulk-flow errors include a contribution from ‘system-matching’ errors which introduce covariance between cluster distance errors (Smith et al. 1997; Hudson et al. 1997).

The large amplitude of the observed flow is initially surprising. We have tested for a wide range of possible systematic effects which might affect this result: no single cluster, or supercluster region, is responsible for the flow; correcting FP distances for stellar population differences, based on the clusters’ offsets from the $\text{Mg}-\sigma$ relation, does not significantly affect the bulk-flow; our choice of Schlegel et al. (1998) extinction maps over Burstein & Hielel (1982) makes little difference to the result; a ‘Method II’ analysis, which fits simultaneously the FP parameters and flow model and is insensitive to Malmquist Bias, yields indistinguishable results.

At face value, the SMAC result appears inconsistent with the bulk-flow solution of Lauer & Postman (1994), whose apex lies $\sim 90^\circ$ from the SMAC flow direction, as well as with the non-detection of bulk-motion in the Tully–Fisher survey of Dale et al. (1999, and these proceedings). In fact, the inconsistencies between surveys are marginal when one accounts for differences in the survey window functions (again see Hudson in this volume). For the same reason, the apparently good agreement between the SMAC and Willick (1999) solutions

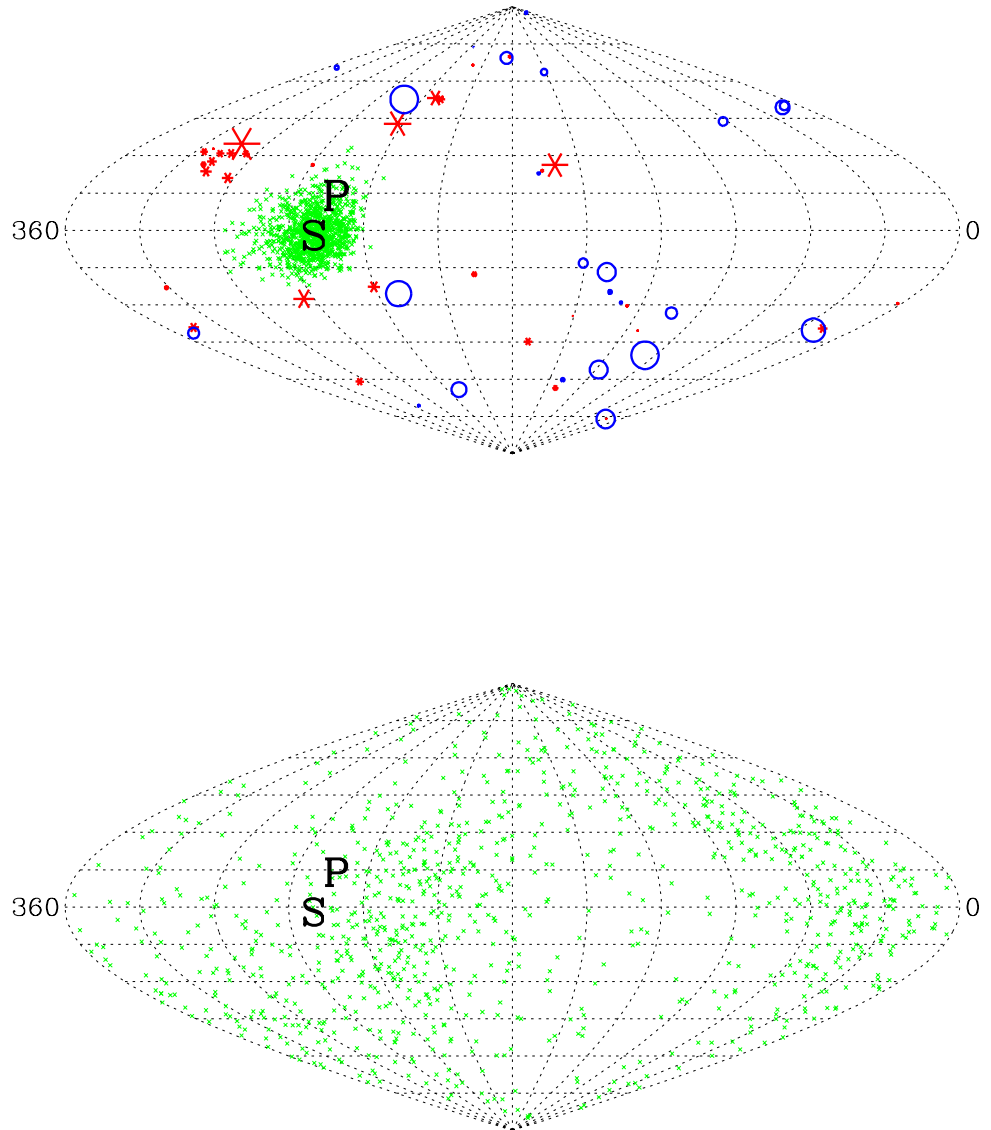


Figure 1. The upper panel shows the sky-projection of the SMAC peculiar velocity field (CMB frame), in galactic co-ordinates. Clusters with positive (negative) peculiar motions are indicated by asterisks (circles), with symbol sizes are assigned according to the magnitude of the cluster peculiar velocity. The **S** indicates the direction of the observed bulk-flow (ie the vector \mathbf{V}_B^{obs}) while **P** shows the PSCz-prediction for the bulk-flow (\mathbf{V}_B^{pred}). The cloud of small crosses show the directional error determined from Monte-Carlo simulations. In the lower panel, we show the bulk-flow direction computed from 1000 Monte-Carlo simulations in which the true cluster velocities are all zero. The preference for directions $b \sim 0^\circ, l \sim 50^\circ, 230^\circ$ results from the relatively poor sampling of this axis by the cluster distribution.

should not be over-interpreted: the surveys have very different window functions, and we should not *expect* the derived bulk-flows to agree so closely!

3. Comparison to IRAS–PSCz

How to interpret the SMAC bulk-flow result depends upon whether the observed velocities of clusters (individually, or combined via the best-fitting bulk-flow model) can be understood as the expected response to the surrounding density field. Here, we compare the SMAC data to density-velocity reconstructions from the most extensive all-sky redshift survey of IRAS galaxies, the PSCz (see contributions of Saunders and Branchini in this volume). The analysis presented here is somewhat preliminary, and various systematic effects remain to be investigated.

First, let us consider the predictions for the bulk-flow. We compute predicted velocities for each of the SMAC clusters (assuming $\beta_I = \Omega_0^{0.6}/b_I = 1$ for now), and substitute these predictions in place of the v_i in Equation 1. We again minimize χ^2 with respect to \mathbf{V}_B , using the same weights computed from the SMAC measurement errors and the thermal velocity noise. The best-fitting flow vector is what PSCz predicts *for the SMAC bulk-flow*, ie. given the SMAC errors and the SMAC sample geometry. Specifically, we fully account for any over-representation of clusters in (for example) the Great Attractor direction. The *expected* bulk-flow solution for $\beta_I = 1$ is then:

$$\mathbf{V}_B^{pred} = [-209, +195, -475] \text{ km s}^{-1}. \quad (3)$$

A cursory comparison between Solutions 2 and 3 reveals that the PSCz velocity field for $\beta_I = 1$, given the SMAC sampling geometry and measurement errors, predicts a best-fitting bulk-flow similar to that observed, (including the large negative SGZ component). Solution 3 has magnitude $490 \pm 140 \text{ km s}^{-1}$ (error-bias corrected) and direction $(l, b) = (253^\circ, 14^\circ)$, which is only $\sim 17^\circ$ from the direction of the observed flow apex (see Figure 1). From Monte-Carlo simulations (lower panel of Figure 1), we find that such a good *directional* agreement arises by chance in $< 3\%$ of realisations.

Alternatively, we can compare directly the predicted and observed velocity fields on a cluster-by-cluster basis, as in Figure 2. The fit yields a measurement of $\beta_I = 0.95 \pm 0.19$, with no individual cluster influencing the result by more than 10%. We can introduce greater freedom into the model velocity field by fitting simultaneously for β_I and a ‘residual’ bulk-flow vector. This residual bulk-flow will absorb any dipole signature *not* accounted for by the PSCz galaxy distribution (either a real streaming generated at very large depths, or a spurious flow resulting from systematic errors). The results of the fit are an unchanged value for $\beta_I = 0.94 \pm 0.25$ and a residual flow vector:

$$\mathbf{V}_B^{resid} = [-169 \pm 103, -117 \pm 110, -170 \pm 190] \text{ km s}^{-1}. \quad (4)$$

The errors are larger than previously since we are now fitting for more parameters; however, the correlation of observed with predicted peculiar velocities remains significant at the $> 3\sigma$ level. That the residual bulk-flow is not significant is a strong indication that the observed SMAC flow is indeed compatible

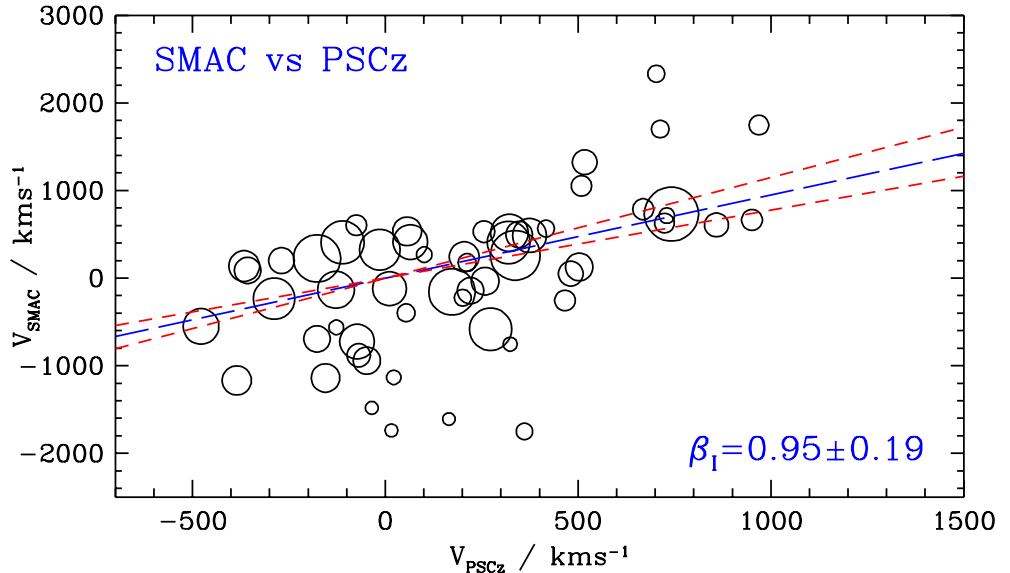


Figure 2. Cluster-by-cluster comparison of SMAC-measured peculiar velocities to the radial peculiar velocities predicted from IRAS–PSCz (for $\beta_I=1$). Symbol sizes are proportional to the weight carried in the fit for β_I . The lines show the best-fitting β_I and its 1σ errors.

with the expected response to local density fluctuations; and suggests that the observed flow does not result primarily from systematic distance errors. The favoured value for β_I is higher than many estimates, but is consistent with other determinations based on PSCz, which yield $\beta_I = 0.6 - 0.7$ (see Branchini, this volume). Note that there is some covariance between β_I and \mathbf{V}_B^{resid} , such that fixing $\beta_I = 0.7$ results in a solution with larger residual flow, albeit significant at only the 1.5σ level.

A final caveat should be noted: the preliminary analysis presented here is based on a Method I approach and is therefore affected by Malmquist Bias. Homogeneous Malmquist effects have been corrected for and the effects of Inhomogeneous Malmquist Bias (IMB) are suppressed by the use of a cluster sample with relatively small distance errors per ‘object’. Nonetheless, it may be expected that the ‘spurious infall’ patterns produced by IMB act to artificially inflate β_I . A crude attempt to judge the effect can be made by removing the 12 clusters with $|v_{PSCz}| > 500 \text{ km s}^{-1}$, which lie mostly in infall regions where IMB will be most severe. The result has much greater uncertainties of course, since we have removed the clusters which contribute the greatest signal-to-noise: we obtain $\beta_I = 0.6 \pm 0.4$, with no measurable residual bulk-flow (amplitude $100 \pm 200 \text{ km s}^{-1}$). In a future analysis of the SMAC–PSCz comparison, we will employ a Method II approach which is free from Malmquist bias effects.

4. The Great Attractor and Shapley Concentration

The SMAC sample includes 10 clusters within 15° of the Shapley / Great Attractor (GA) direction (visible in Figure 1 as the concentration of points at $l = 315^\circ, b = 30^\circ$). Since this region is of some historical interest, we compare in Figure 3 the observed velocities with some (over-)simplistic toy-models for the dynamics of the region. The models are based upon the simple spherical attractors of Faber & Burstein (1988). We consider the effect of two such structures, one at the position of the ‘traditional’ GA (at a distance of 4500 km s^{-1}) and a second centered on the Shapley core region (at 14500 km s^{-1}). The models are normalised to generate the GA-directed component of the Local Group’s velocity in the CMB frame, viz. 500 km s^{-1} .

The leftmost panel of Figure 3 demonstrates that a pure GA infall model is a poor fit to the SMAC data, especially in the immediate GA background, where no ‘far-side infall’ is observed. Equally, the extreme Shapley infall model dramatically over-predicts velocities beyond $\sim 10000 \text{ km s}^{-1}$ (middle panel). Allowing for contributions from both attractors, and fitting for their relative amplitudes as the single free parameter, we can obtain an acceptable fit to the data, as shown in the rightmost panel. The best-fitting model has Shapley and the GA each generating $50 \pm 10\%$ of the Local Group velocity in this direction, proportions which accord with Hudson’s (1994) conclusions based on the Mark II dataset.

Here, as in the case of ‘bulk-flow’ we caution against drawing quantitative conclusions from analyses based on unrealistically simple models of the velocity field. However, the above fits draw attention to the qualitative behaviour of the SMAC velocity data in the GA / Shapley direction. The absence of far-side infall in the SMAC data (here visualised as a retardation of one infall pattern by another more distant infall structure) is also apparent in the PSCz maps, which reveal a wealth of structure along the GA-Shapley axis.

5. Conclusions

From our analyses of the SMAC velocity field, as presented in the preceding sections, we draw the following conclusions:

1. The best-fitting bulk-flow model has amplitude $640 \pm 200 \text{ km s}^{-1}$, towards $(l, b) = (260^\circ, -2^\circ)$.
2. The direction of the observed bulk-flow is within $\sim 15^\circ$ of the direction predicted from the IRAS–PSCz redshift survey for the SMAC sample, while the amplitude can be matched if $\beta_I \sim 1$.
3. Comparing observed and predicted velocities cluster-by-cluster yields $\beta = 0.95 \pm 0.25$, compatible with other analyses based on the PSCz.
4. The observed velocity field is fully accounted for by the local density field, with no recourse to residual flow generated beyond the limits of PSCz, or to ‘spurious’ flows associated with systematic errors.

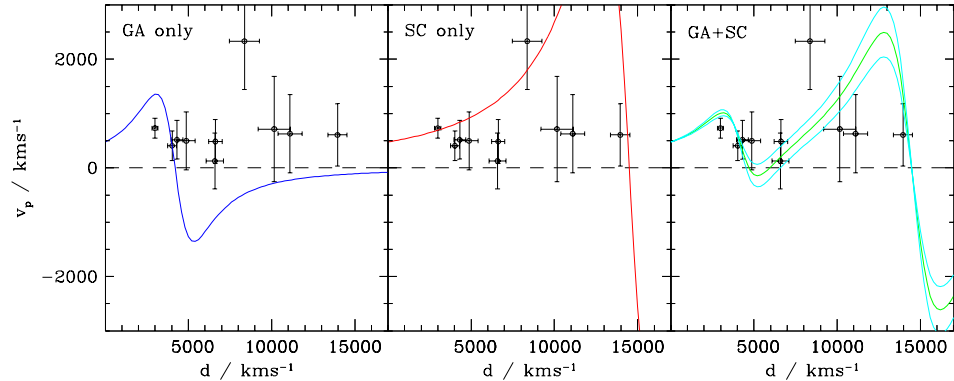


Figure 3. SMAC peculiar velocities in the Great Attractor / Shapley direction. The data are identical in each panel. The models shown are: a spherically symmetric Great Attractor model (left); a similar model attractor at Shapley (middle); the best fitting ‘two-attractor’ model, with errors (right). All models are normalized to generate 500 km s^{-1} at the Local Group.

5. The Shapley Concentration may be responsible for a significant fraction of the infall traditionally associated with the Great Attractor.

Acknowledgments. We thank Enzo Branchini, Carlos Frenk and the PSCz team for allowing us to discuss collaborative work in advance of publication.

References

- Burstein D., Heiles C. 1982, *AJ*, 87, 1165
Dale D. A., Giovanelli R., Haynes M. P., Campusano L. E., Hardy E., Borgani S., *ApJ*, 510, L11
Faber S. M., Burstein D., 1988, in Coyne G., Rubin V. C., eds, *Proceedings of the Vatican Study Week, Large Scale Motions in the Universe*. Princeton Univ. Press, Princeton, p. 135
Feldman H. A., Watkins R. 1994, *ApJ*, 430, L17
Hudson M. J. 1994, *MNRAS*, 266, 468
Hudson M. J., Lucey J. R., Smith R. J., Steel J. 1997, *MNRAS*, 291, 488
Hudson M. J., Smith R. J., Lucey J. R., Schlegel D. J., Davies R. L. 1999, *ApJ*, 512, L79
Lauer T. R., Postman M. 1994, *ApJ*, 425, 418
Schlegel D. J., Finkbeiner D. P., Davis M. 1998, *ApJ*, 500, 525
Smith R. J., Lucey J. R. Hudson M. J., Steel J. 1997, *MNRAS*, 291, 461
Willick J. A. 1999, *ApJ*, submitted (astro-ph/9812470)